Combined Ash and Soot Monitoring for Gasoline Particulate Filters Using a Radio-Frequency-Based Sensor

Stefanie Walter[1] · Peter Schwanzer[2] · Gunter Hagen[1] · Hans-Peter Rabl[2] · Markus Dietrich[3] · Ralf Moos[1]

Abstract

Increasingly stringent emission limits have made particulate filters necessary for gasoline engines. Similar to diesel applications, gasoline particulate filters (GPFs) can be monitored by differential pressure measurement or by the radio-frequency-based filter diagnosis (RF sensor). In addition to measuring the soot loading, ash detection is critical for monitoring the GPF over the entire vehicle lifetime. Because the RF sensor detects the filter loading through a change in the dielectric properties of the GPF, it can detect not only soot but also ash. In diesel applications, the RF sensor has already demonstrated its potential for ash detection. To verify the feasibility of simultaneous ash and soot monitoring for GPFs, filters were loaded with ash on an engine test bench and measured on a lab test bench under defined synthetic exhaust gas conditions. By evaluating resonant modes, soot and ash could be clearly distinguished, as ash mainly affects the resonant frequency, while soot also changes the quality factor due to its high dielectric losses. However, higher soot loadings could not be detected by the resonant parameters, but instead by a frequency-averaged transmission signal. While the presence of ash caused an offset in this signal, its sensitivity to soot was not affected. Thus, the influence of ash can be corrected if the signal in the soot-free filter state is known, e.g., from the behavior of the resonant parameters. Therefore, even with a continuously increasing ash loading over the lifetime of a vehicle, an accurate soot detection is possible with the RF sensor.

Keywords Gasoline particulate filter (GPF) · Radio-frequency (RF) · Soot mass determination · Ash detection

1 Introduction

While diesel vehicles have been equipped with particulate filters as standard for many years, particulate filters for gasoline direct injection (GDI) engines have only become necessary due to the recent limitation of the number of particles emitted in addition to the previously limited mass of particles [1]. These stricter regulations, which will be further tightened in the European Union with the introduction of the Euro 7 emission standards in the coming years, have been introduced because recent studies have shown that in terms of adverse health effects, the particle number is more relevant than the particle mass [2–5]. As a consequence, the majority of GDI vehicles in production today are now equipped with gasoline particulate filters (GPFs), in which the soot particles emitted by the engine can be trapped and oxidized during regeneration phases [6, 7].

In addition to soot, particulate filters also trap other particles such as ash. Ash particles are any inorganic, non-oxidizable particles present in the exhaust gas. The primary sources of ash are the additives in the engine oil [8]. Small amounts also originate from fuel additives, metallic wear in the engine, and detached catalyst material [8]. Unlike soot particles, ash trapped in the particulate filter cannot be removed by oxidation and therefore accumulates over the life of the vehicle. Several studies on gasoline vehicles with more than 160,000 km have shown that 0.14 to 0.25 mg/km of ash is generated and stored in the filter [7, 9–11]. This ash accumulates in the GPF mainly in the walls of the inlet channels. However, some of the ash is also found in plugs at the ends of the channels, although these ash plugs are significantly shorter than in DPF applications, with a length of 10 mm, even at high ash loadings of more than 30 g/l$_{\text{GPF}}$ [8–10]. As

✉ Ralf Moos
    Functional.Materials@uni-bayreuth.de

[1] Bayreuth Engine Research Center (BERC), Department of Functional Materials, University of Bayreuth, 95447 Bayreuth, Germany

[2] Ostbayerische Technische Hochschule Regensburg, 93053 Regensburg, Germany

[3] Vitesco Technologies GmbH, 93055 Regensburg, Germany

a result of the ash particles accumulating in the filter pores, the differential pressure behavior of the filter, which according to the start of the art is used to monitor the soot loading, changes. On the one hand, the ash increases the differential pressure, although the mass-related pressure increase is less than for soot loading [8, 12]. On the other hand, the ash in the GPF allows less soot to be deposited in the filter pores, thus reducing the large pressure increase resulting from depth filtration [13]. These effects can reduce the accuracy of differential pressure-based load monitoring, which is required for an error-free operation of the particulate filter [9].

In previous studies, an alternative approach to monitor the soot loading of GPFs was presented with the radio-frequency-based filter diagnosis (RF sensor) [14–17]. With this sensor, deposited soot is detected by its dielectric properties. Other particles, such as ash, can also be detected if they cause a change in the effective dielectric properties of the particulate filter system. For DPFs, the general feasibility of ash monitoring has already been demonstrated [18]. However, it is not yet clear whether these results can be transferred to gasoline ash, as the ash is distributed differently in the particulate filter, which may affect the sensitivity of the RF sensor due to the local distribution of the electric field [19]. It is also unclear whether the soot detection is affected by the presence of ash. In addition, it is to be investigated in which way the RF sensor signals can be evaluated in order to realize a simultaneous monitoring of soot and ash loading. For this purpose, particulate filters are loaded with ash on the engine test bench according to the procedure described in [20] until the amount of stored ash represents a typical end-of-life loading of a vehicle. These filters are then characterized on the lab test bench regarding their influence on the RF sensor compared to an unloaded particulate filter. In addition, to analyze the cross-influence of ash on soot detection, these filters are loaded with synthetic soot and the resulting sensitivity of the RF sensor is compared to that of ash-free particulate filters.

2 Fundamentals of the Radio-Frequency-Based Loading Detection

The detection of soot and ash loading by the RF sensor is possible due to the change in the effective dielectric properties of the particulate filter as a result of the deposition of particles. The dielectric properties can be described by the complex relative permittivity ε_r with the ε_r' as the real part and the dielectric losses ε_r'' (imaginary part), which are caused not only by polarization losses $\varepsilon_{r,pol}''$ but also by conductivity losses σ (Eq. (1)). The latter also depends on the vacuum permittivity ε_0 and the angular frequency of the excited electromagnetic field $\omega = 2\pi f$.

$$\varepsilon_r = \varepsilon_r' - j\varepsilon_r'' = \varepsilon_r' - j\left(\varepsilon_{r,pol}'' + \frac{\sigma}{\varepsilon_0\omega}\right) \tag{1}$$

The RF sensor can detect changes in the electromagnetic properties of the filter as they affect the propagation of the electromagnetic waves excited by the sensor within the particulate filter. The electromagnetic waves are usually excited by coupling elements such as antennas. At the same time, between the two antennas of the RF sensor, the frequency spectrum of the transmission factor $|S_{21}|$ can also be measured. This allows the propagation behavior of the electromagnetic waves to be studied. Since the electromagnetic waves are excited within the metallic canning of the particulate filter, standing waves can form in the cavity due to mutual superposition. The resulting resonant modes can be described by the resonant frequency f_{res} and the quality factor Q_0. These parameters are evaluated in this paper based on the $|S_{21}|$ spectra using the same methods as in [16, 21]. According to the microwave cavity perturbation (MCP) method, inserting a sample into a resonant cavity results in a change of its resonant frequency Δf_{res}, which is related to the relative permittivity of the sample ε_r' (Eq. (2)), while a shift of the inverse quality factor ΔQ^{-1} can be attributed to the dielectric losses ε_r'' (Eq. (3)) [22, 23].

$$\Delta f_{res} \sim \varepsilon_r' \tag{2}$$

$$\Delta\left(Q_0^{-1}\right) \sim \varepsilon_r'' \tag{3}$$

Direct measurement of the dielectric properties of a GPF installed in an exhaust gas system, and thus of soot and ash, using the MCP is challenging due to several unknown influencing factors, including the exact temperature distribution across the filter and the inability to calibrate with an empty filter canning. In addition, the particulate filter fills a large portion of the canning, preventing the application of the MCP, which requires the investigated sample to be small relative to the resonant cavity, without employing extensive correction terms [23]. Although the value of the dielectric properties cannot be calculated using the MCP, the general correlations from Eqs. (2) and (3) still apply to the setup investigated in this work. In particular, a change in the resonant frequency can be attributed to a change in the permittivity of the particulate filter, and a change in the quality factor can be attributed to changing dielectric losses [21]. Therefore, the resonant frequency f_{res} and the quality factor Q_0 can be used as a signal to detect the soot loading [16]. It can be expected that ash deposition also affects the dielectric filter properties and thus the resonant parameters. Whether this effect is strong enough to determine the ash loading will be investigated in this work.

From previous studies on soot-loaded particulate filters, it is known that due to the conductivity of the soot, it is no

longer possible to evaluate resonances above a certain soot loading [24]. However, the $|S_{21}|$ signal averaged over a wide frequency range can be used to continue the soot loading detection [17, 24–27]. As with the resonant parameters, it can be assumed that the ash loading can influence the averaged $|S_{21}|$ signal, and therefore the RF sensor will need to take this into account for a correct monitoring of the soot loading.

3 Methodology

3.1 Method to Generate Engine Ash

Due to the usually small amounts of ash generated during normal engine operation, the ash investigated in this paper was produced on an engine test bench using the method described in [20]. Thereby, the amount of oil burned in the engine is increased by an active oil injection into the intake manifold, which leads to an ash generation of 1.2 g/h and therefore compared to real ash production faster up to a factor of 100. Here, the Fuchs Titan GT1 Pro C3 in viscosity grade 5W-30 is used, the same engine oil that is also used to operate the engine. This has an ash content of 0.736 w.-%, whereby the most frequently occurring elementary components are sulfur (1828 mg/kg), calcium (1551 mg/kg), and zinc (852 mg/kg) [20]. The engine is operated at medium speed and low engine load (3500 rpm and 32.5% load), and the temperature upstream of the GPF is 585 °C at this operating point. The resulting particles are deposited in a GPF whose cordierite substrates are supplied by Corning. The cordierite substrates have a length of 5″ (127 mm), a diameter of 5.2″ (132 mm), a cell density of 200 cpsi, and a wall thickness of 8.5 mil (215.9 μm). The filters are designed for gasoline engine vehicles and do not have a catalytic active coating. For further investigations, cores with a diameter of 48 mm and therefore a volume of 0.23 l were cut from the filter and mounted in cannings with an inner diameter of 50 mm using a mounting mat. This enables tests on a lab test bench under defined conditions regarding filter temperature and exhaust gas composition. The ash produced was deposited uniformly on the filter walls of the inlet ducts, as can be seen in Fig. 1 on a filter opened along the channels. In addition, some of the ash forms a plug with a length of several millimeters at the end of the channel. Such an ash distribution is also observed in natural ash loading of GPF applications [10, 28].

For the experiments in this work, filters with an ash loading m_{ash} of 27.6 g/l in relation to the filter volume were used. This was determined by weighing the filter before and after loading and corresponds to a typical loading at the end of a vehicle lifetime [7, 10]. Throughout the entire ash
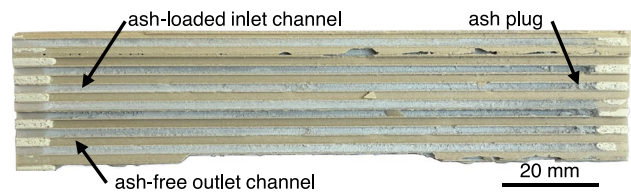

Fig. 1 Image of a GPF loaded with 27.6 g/l engine ash. The GPF has been cut along the inlet and outlet channels

generation, a total of 48 g of ash was introduced into the particulate filter. Based on a typical generation rate of up to 0.25 mg/km, this amount corresponds to a driving distance of at least 192,000 km [7, 9–11].

3.2 Loading the Ash-Loaded Filter with Synthetic Soot

To analyze the influence of ash on the soot loading detection of the RF sensor, the ash-loaded particulate filters were subsequently loaded with soot. Loading on an engine test bench was not an option because the dielectric properties of the soot generated there can vary widely [24]. Instead, to ensure comparability between differently loaded samples, they are loaded with the synthetic soot PrintexU (manufactured by Orion Engineered Carbons), which is often used as a surrogate for gasoline soot particles in automotive applications [29, 30]. The values of both the permittivity and the dielectric losses, respectively, the conductivity of PrintexU, are generally at the lower end compared to those of real engine soot [24]. The model soot is deposited into the filter using a powder gun, which can be connected directly to the used filter cannings as shown in Fig. 2. The PrintexU particles are fluidized in an aerosol flask using a nitrogen carrier gas flow of 10 l/min for all loadings set by a mass flow controller (MFC). Nitrogen also served as the shear flow gas. Its volume flow was generated by applying an overpressure of 4 bar to the powder gun inlet. Through the Venturi nozzle, the shear flow in the aerosol bottle generated a negative pressure of 55 mbar compared to ambient air, whereby the PrintexU particles were sucked into the nozzle. The shear gas flow then transported them into the particulate filter, where they were deposited as the gas flows through the filter walls. Thereby, the soot is deposited evenly over the entire length of the inlet channels in the filter, as is the case with soot loads in real-world applications [31, 32].

The PrintexU in the aerosol bottle of the powder gun was completely transferred into the particulate filter, except for some larger agglomerates, which were formed by static charging in the fluidized bed. The soot loading present in the filter was determined by weighing the sample before and after the addition of the synthetic soot. To reduce the possible influence of moisture, the samples were stored in a drying oven

Fig. 2 Powder gun "Bengs Modellbau NP-09-EU" used for loading the GPF drill cores with synthetic soot. A 3D-printed adapter was used for a tight connection with the filter canning
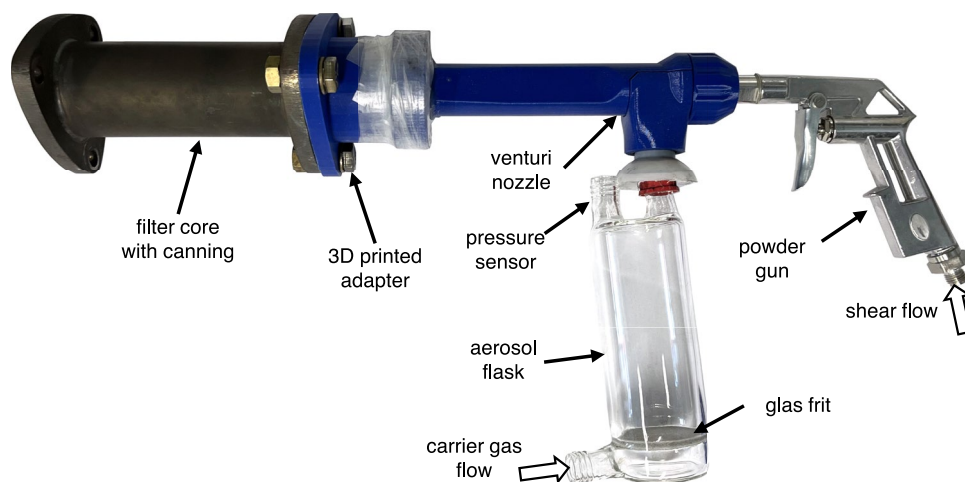
at 120 °C for at least 24 h before weighing. As determined in [24], these weightings are subject to an error of up to 5%.

3.3 Examination of the Influence of Ash and Soot on the RF-Sensor

To analyze the effects of ash and soot loading on the RF sensor under defined conditions, the setup shown in Fig. 3(a) was used. The filter cores were continuously flushed with 40 l/min nitrogen provided. The antennas required for measuring the radio-frequency properties are located in adapter pieces connected to the canning. An ideal cylindrical resonator geometry with a length of 295 mm is defined by the perforated grids installed on the inlet and outlet sides. In order to investigate the GPF at different temperatures, the exhaust gas was heated up to 600 °C by an in-line heater before passing through the GPF. Heat losses through the outer walls of the cannings were reduced by heating elements installed there. This resulted in a maximum temperature gradient of 5 K between the thermocouples located outside of the resonator geometry during stationary operation. Owing to this small difference, the filter temperature T_{GPF} is defined as the average of the temperatures measured by the thermocouples.

Figure 3(b) shows the spectra of selected filter samples at a temperature of 400 °C. Despite the high ash mass of 27.6 g/l, the resonant maximum is not significantly more attenuated compared to the soot- and ash-free filter. However, the resonant frequency is shifted to lower frequencies due to the permittivity of the deposited particles. The situation is different for the sample loaded with 0.5 g/l PrintexU (no ash). Although a shift of f_{res} can also be observed here, the conductive synthetic soot causes additionally a drop of more than 5 dB in the maximum transmission signal, resulting in a change in the inverse quality factor Q_0^{-1}. Therefore, the resonant parameters (f_{res} and Q_0^{-1}) can be used to distinguish between soot and ash as long as only a small amount of soot is present in the particulate filter. At higher loadings the resonant parameters can no longer be reliably evaluated since the signal is too much attenuated [24]. To nevertheless allow soot detection using the RF sensor, an averaged transmission signal $S_{21,m}$ in the frequency range from 3.3 to 3.5 GHz was used (Eq. (4)). The sensor behavior determined on filter cores can, in principle, also be transferred to lower frequency ranges for the monitoring of complete particulate filters [33].
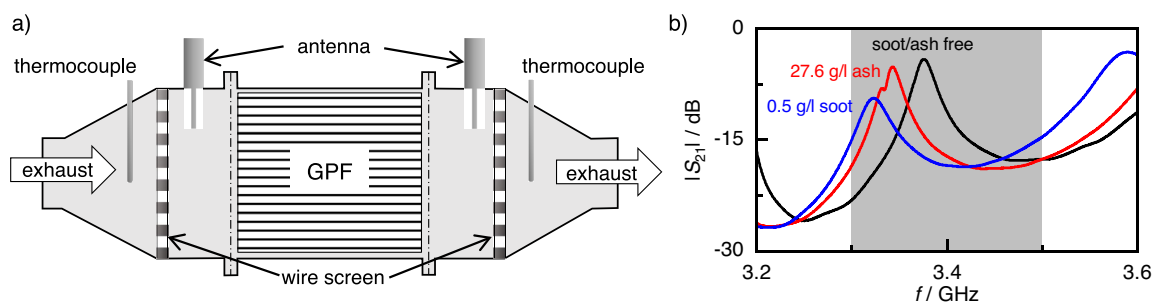

Fig. 3 **a** Schematic illustration of the measurement setup for the evaluation of the filter cores on the lab test bench. **b** Transmission signal |S21| of a soot- and ash-free, an ash-loaded (27.6 g/l) and a soot-loaded (0.5 g/l PrintexU) filter core at 400 °C versus frequency *f*. The |S21| signal averaged over the gray-shaded frequency range from 3.3 to 3.5 GHz is used as the $S_{21,m}$ signal of the RF sensor
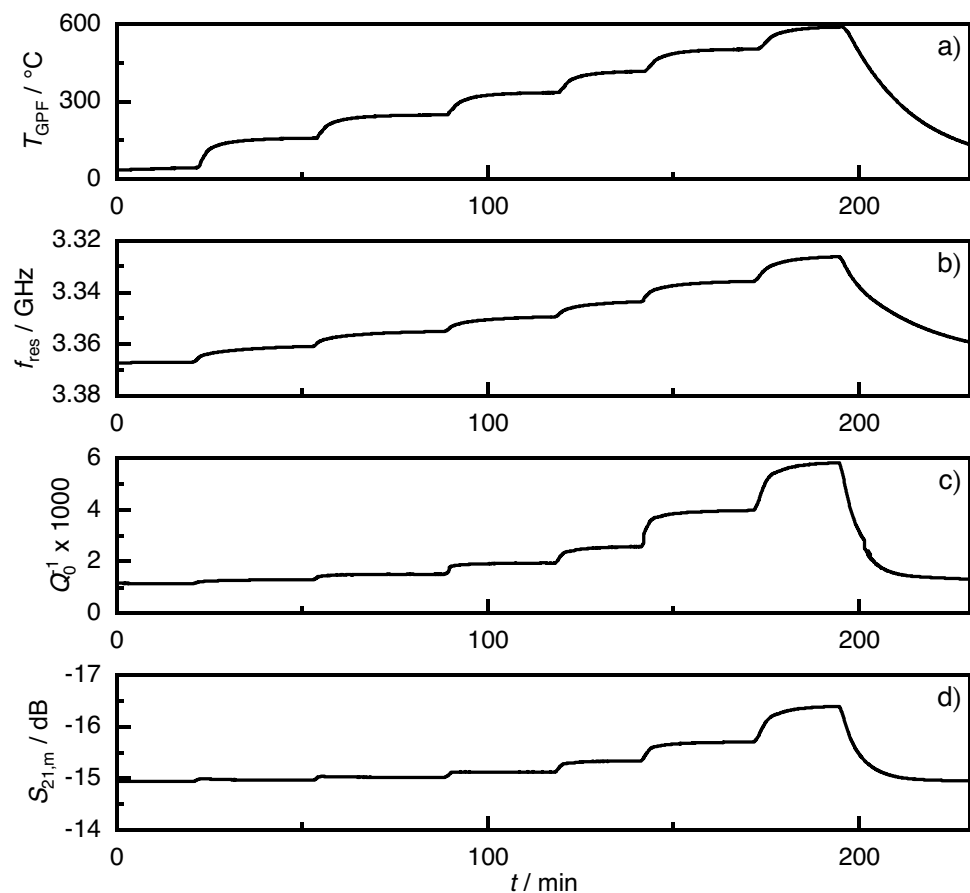
$$S_{21,m} = \sum_{3,3\text{GHz}}^{3,5\text{GHz}} 20 \cdot \log_{10}|S_{21}(f)| \qquad (4)$$

To determine the temperature-dependent behavior of ash and soot, all filter cores are heated from room temperature to 600 °C in several steps. The measurement procedure for an ash-loaded filter is shown in Fig. 4. To analyze the sensor behavior in detail, the RF signals are then evaluated after each stationary temperature is reached.

4 Ash Loading Detection Using the RF-Sensor

In the following, it will be examined whether the ash introduced into the filter cores causes a sufficiently strong shift of the resonant parameters to be able to detect the ash loading with the RF sensor. In addition, it is unknown whether ash affects the sensitivity of the RF sensor to soot s_{soot}. To check for this effect, particulate filters with and without ash loading were loaded with synthetic soot.

4.1 Ash Detection in Soot-Free Particulate Filters

Since the ash loading was carried out on full filters and the measured cores were cut out from them afterward, it was not possible to make a direct comparison measurement with the same filter core in an ash-free state. Nevertheless, the basic influence of ash on the RF sensor can be evaluated, since in the unloaded state the filter core samples differ only slightly between different samples with regard to the resonant parameters and the average signal attenuation $S_{21,m}$. To illustrate this, the RF signal of 10 unloaded filter cores was measured. Their resulting average temperature-dependent signals are shown in Fig. 5 regarding f_{res} and Q_0^{-1} and in Fig. 6 regarding $S_{21,m}$ including the corresponding standard deviation. In addition, two measurements of filters loaded with 27.6 g/l ash are shown in Fig. 6. These data were determined first in a soot-free condition and later after the ash-loaded filter had been additionally loaded with 0.5 g/l PrintexU.

The ash loading of 27.6 g/l reduces the resonant frequency f_{res} by about 25 MHz compared to the unloaded state, which is more than twice the standard deviation of the unloaded filter signal. The additional soot loading of 0.5 g/l PrintexU then leads to a further resonance shift of 6 MHz. In contrast, the effect of ash on the quality factor
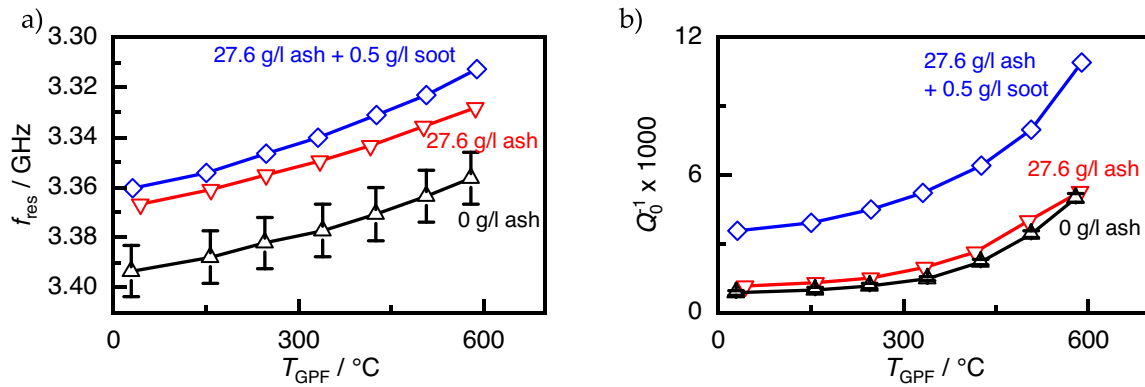
Fig. 4 Stepwise heating of a filter core loaded with 27.6 g/l ash. Besides the filter temperature T_{GPF} (a) the corresponding signals of the RF sensor (b: resonant frequency f_{res}, c: inverse quality factor Q_0^{-1} and d: averaged transmission signal $S_{21,m}$) are shown

Fig. 5 Resonant frequency f_{res} (**a**) and inverse resonant quality Q_0^{-1} (**b**) of a filter with 27.6 g/l ash loading in a soot-free and soot-loaded state and the mean value of 10 soot- and ash-free cores examined, indicating the associated standard deviation as a function of the filter temperature T_{GPF}
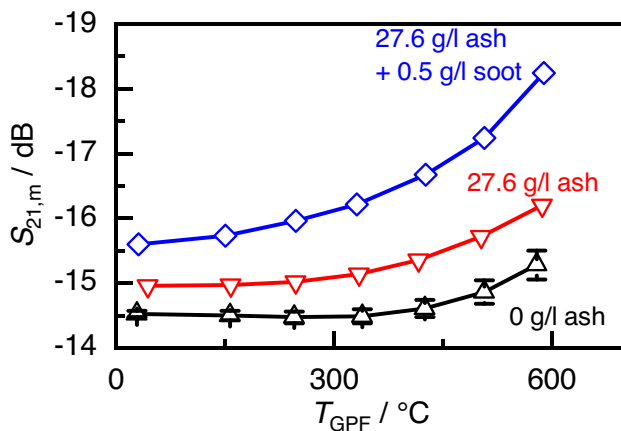

Fig. 6 Signal attenuation $S_{21,m}$ of a filter with 27.6 g/l ash loading in a soot-free and soot-loaded condition and the average value of 10 soot- and ash-free cores with indication of the associated standard deviation as a function of the filter temperature T_{GPF}

is weak compared to the influence of soot. Nevertheless, a significant increase in Q_0^{-1} can be measured compared to the unloaded samples. In comparison, assuming a linear relationship between Q_0^{-1} and the stored particle mass, the quality factor is affected by 27.6 g/l ash to the same extent as by only 60 mg/l soot, indicating much lower dielectric losses for ash compared to soot (cf. Equation (3)). Since the resonant frequency and the quality factor react quite differently to the ash loading, it is possible to distinguish between soot and ash loading with the RF sensor. The simultaneous detection of two different components has already been demonstrated for NO_x storage catalysts regarding their NO and O_2 loading [34]. Up to which soot loading soot and ash can be detected simultaneously via the resonant parameters cannot be generally determined. In [24], the resonance parameter evaluation was possible for drill cores with 0.7 g/l real engine soot, but became unfeasible at a loading

of 1.5 g/l. The exact limit, however, depends on numerous parameters such as the geometry of the exhaust tract, the dielectric soot properties, or the evaluated resonant mode.

To determine the soot loading, the averaged attenuation signal $S_{21,m}$ is more important in regular operation because, unlike the resonant parameters, it can be evaluated even at high soot loading. However, this signal is also influenced by the ash loading, whereby both permittivity (which mainly causes the shift in f_{res}) and dielectric losses (causing the shift in Q_0^{-1}) are relevant for the resulting signal shift. Ash of 27.6 g/l causes an about 0.5 dB higher attenuation. This shift is almost independent of temperature and exceeds the standard deviation of the unloaded signal by a multiple (Fig. 6). Thus, the sensitivity of the RF sensor to ash is about 0.02 dB/(g/l), assuming linear behavior. By loading this filter with an additional 0.5 g/l PrintexU, the attenuation increases further. This effect is more pronounced at higher temperatures. This temperature-dependent behavior has already been observed in ash-free particulate filters and is caused by the dielectric properties of soot [24]. At 400 °C, which is a typical operating temperature for GPFs [10], the synthetic soot leads to a sensitivity of the RF sensor of about 3 dB/(g/l), which is therefore 150 times higher than the sensitivity caused by ash. The present ash loading would therefore cause the same change in attenuation as a loading with 0.18 g/l PrintexU. Therefore, in order to properly detect the soot loading and in particular the soot-free filter condition, the signal attenuation must be corrected by an offset dependent on the ash loading.

4.2 Influence of Ash on the RF-Based Detection of the Soot-Loading

Finally, the question arises whether the ash loading only affects the zero point of the RF sensor or also its sensitivity to soot. The dependency of the resonant frequency and the

quality factor on the soot loading will not be considered further in this section because, due to the increasing signal attenuation, they can only be evaluated for the samples with the lowest soot loading. Based on the signal attenuation $S_{21,m}$, its sensitivity to soot s_{soot} can be determined using Eq. (5), since $S_{21,m}$ changes linearly with the soot loading of the particulate filter [35]. Since the temperature T_{GPF} at the stationary measuring points differs slightly between the samples, the difference in the attenuation signal between the loaded and unloaded filter states, which is necessary to calculate s_{soot}, cannot be calculated directly. Instead, the temperature-dependent signal of the soot-free drill core is described by a 3rd degree polynomial fitted to the measured data by the method of least squares. This is then used to determine the attenuation signal of the unloaded filter $S_{21,m}(m_{soot} = 0\,g/l)$ at the corresponding measurement temperatures of the loaded filters.

$$s_{soot} = \frac{S_{21,m} - S_{21,m}(m_{soot} = 0\,g/l)}{m_{soot}} \tag{5}$$

To analyze the influence of ash on s_{soot}, an ash-loaded filter core was loaded with three different amounts of the synthetic soot PrintexU. With the same procedure, s_{soot} was also determined for an ash-free filter (Fig. 7). For the three different PrintexU loadings, the sensitivity is almost identical for both the ash-free and the ash-loaded filter. Only at the lowest loading of 0.46 g/l and 0.51 g/l, respectively, s_{soot} is slightly lower in both cases. Nevertheless, these measurements confirm that the basic linear relationship between $S_{21,m}$ and the soot loading m_{soot} is still present even for ash-loaded particulate filters. In addition, the sensitivity of the RF sensor is almost unchanged despite the ash loading. Thus, even with the high ash loading at the end of the vehicle lifetime, no change in the RF sensor behavior with respect to soot detection is expected.

Consequently, in order to correctly detect the soot loading over the entire life of the vehicle, the continuously increasing ash loading has only to be considered by a zero-point correction. No adjustment of the RF sensor sensitivity is required. The offset correction can be performed by evaluating the attenuation signal of a soot-free filter. The absence of soot can be ensured, for example, by a sufficiently long regeneration phase. In this case, it would not be necessary to determine the sensitivity of the RF sensor to ash in advance. However, if this is known, the ash and soot loading of the GPF can be determined separately by evaluating the resonant parameters using the method described in [34].

5 Conclusions

Due to the different operating conditions, it is more difficult to monitor the ash and soot loading of GPFs than of diesel particulate filters using conventional differential pressure sensors. Therefore, the RF sensor was developed as an alternative. While previous studies [14, 24] have focused on its soot monitoring behavior, this work investigated the feasibility of the RF sensor to detect ash loading simultaneously with a present soot loading, as well as whether ash affects the soot detection.

For this purpose, GPFs were loaded with ash on an engine test bench using the method described in [20]. To investigate the effect of ash on the soot detection, the filters were subsequently loaded with the synthetic soot PrintexU. Measurements on a lab test bench have shown that an ash loading without soot loading primarily shifts the resonant frequency, while an additional soot loading mostly attenuates the RF signal and thus reduces the quality factor, while having only a small effect on the resonant frequency. A typical ash loading at the end of a vehicle's lifetime has the same effect on the quality factor as a soot loading of only 0.06 g/l, while the resonant frequency shift is equivalent to a loading of more than 1 g/l. Because of this different response, a distinction between soot and ash loading can be made using a method similar to that used in [34].

However, this approach is only applicable for low soot loadings, since otherwise the high conductivity of the soot impedes the evaluation of the resonant parameters. For this reason, the transmission signal averaged over a wide frequency range $S_{21,m}$ is typically used to determine the soot loading. While this signal is also affected by the ash loading,

Fig. 7 Sensitivity of the RF sensor s_{soot} to the soot mass deposited in the filter for different PrintexU and ash loadings as a function of the filter temperature T_{GPF}; **a** 0 g/l ash as well as 0.46 g/l, 1.57 g/l, and 1.90 g/l PrintexU; **b** 27.6 g/l ash as well as 0.51 g/l, 1.25 g/l, and 2.14 g/l PrintexU
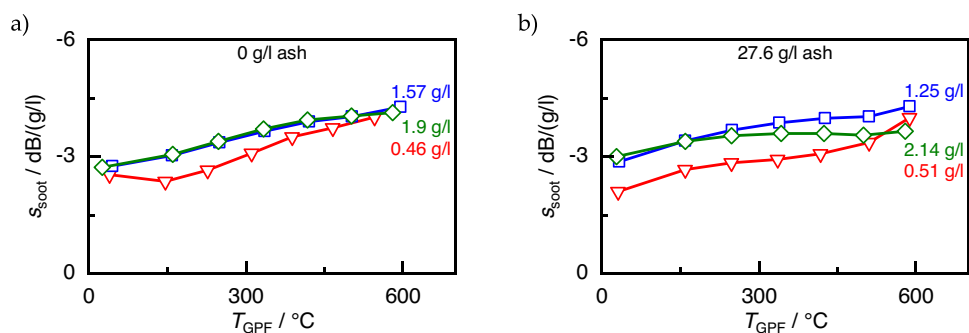
its sensitivity to ash is, as for the quality factor, much lower than that to soot. Nevertheless, ignoring ash could lead to an error of up to 0.2 g/l in determining the soot loading. Since no influence of the ash on the sensitivity of the RF sensor can be observed, this can be compensated by a zero-point correction. For this purpose, only the RF signal of the soot-free filter needs to be known, which can be achieved, for example, by sufficiently long regeneration phases or by evaluating the resonant parameters.

Author Contribution S.W., P.S., C.S., G.H., H.-P.R., M.D., and R.M. conceived the experiments. M.D. provided the filter samples. P.S. performed the ash loading on the engine test bench. S.W. performed the lab test bench experiments. All together analyzed the data, evaluated and discussed the results, and wrote the paper.

Data Availability All relevant data presented in the article are stored according to institutional requirements and as such are not available online. However, all data used in this paper can be made available upon request to the authors.

Declarations

Competing Interests The authors declare no competing interests.

References

1. Platt, S.M., El Haddad, I., Pieber, S.M., et al.: Gasoline cars produce more carbonaceous particulate matter than modern filter-equipped diesel cars. Sci. Rep. **7**, 4926 (2017). https://doi.org/10.1038/s41598-017-03714-9

2. Hennig, F., Quass, U., Hellack, B., et al.: Ultrafine and fine particle number and surface area concentrations and daily cause-specific mortality in the ruhr area, Germany, 2009–2014. Environ. Health Perspect. **126**, 27008 (2018). https://doi.org/10.1289/EHP2054

3. Peters, A., Rückerl, R., Cyrys, J.: Lessons from air pollution epidemiology for studies of engineered nanomaterials. J. Occup. Environ. Med. **53**, 8–13 (2011). https://doi.org/10.1097/JOM.0b013e31821ad5c0

4. Hofman, J., Staelens, J., Cordell, R., et al.: Ultrafine particles in four European urban environments: results from a new continuous long-term monitoring network. Atmos. Environ. **136**, 68–81 (2016). https://doi.org/10.1016/j.atmosenv.2016.04.010

5. Rivas, I., Vicens, L., Basagaña, X., et al.: Associations between sources of particle number and mortality in four European cities. Environ. Int. **155**, 106662 (2021). https://doi.org/10.1016/j.envint.2021.106662

6. Lanzerath, P., Wunsch, R., Schön, C. (2017). The first series-production particulate filter for Mercedes-Benz gasoline engines. In: Bargende, M., Reuss, HC., Wiedemann, J. (eds) 17. Internationales Stuttgarter Symposium. Proceedings. Springer Vieweg, Wiesbaden. https://doi.org/10.1007/978-3-658-16988-6_68

7. Joshi, A., Johnson, T.V.: Gasoline particulate filters—a review. Emiss. Control. Sci. Technol. **4**, 219–239 (2018). https://doi.org/10.1007/s40825-018-0101-y

8. Coulet, B., Rose, D., Boger, T., et al.: Ottomotoren mit Partikelfilter Erfahrungen zur Ascheeinlagerung und Auswirkungen auf die Filtereigenschaften. Motortech. Z. **80**, 46–51 (2019). https://doi.org/10.1007/s35146-018-0137-0

9. Custer, N., Kamp, C.J., Sappok, A., et al.: Lubricant-derived ash impact on gasoline particulate filter performance. SAE Int. J. Engines **9**, 1604–1614 (2016). https://doi.org/10.4271/2016-01-0942

10. Lambert, C., Bumbaroska, M., Dobson, D., et al.: Analysis of high mileage gasoline exhaust particle filters. SAE Int. J. Engines **9**, 1296–1304 (2016). https://doi.org/10.4271/2016-01-0941

11. Ito, Y., Shimoda, T., Aoki, T., et al.: Next generation of ceramic wall flow gasoline particulate filter with integrated three way catalyst. SAE Tech. Pap. (2015). https://doi.org/10.4271/2015-01-1073

12. Shimoda, T., Ito, Y., Saito, C., et al.: Potential of a low pressure drop filter concept for direct injection gasoline engines to reduce particulate number emission. SAE Tech. Pap. (2012). https://doi.org/10.4271/2012-01-1241

13. Nowak, D.: Ruß- und Aschedeposition in Ottopartikelfiltern. Springer Fachmedien Wiesbaden, Wiesbaden (2018)

14. Walter, S., Schwanzer, P., Hagen, G., et al.: Modelling the influence of different soot types on the radio-frequency-based load detection of gasoline particulate filters. Sensors **20**, 2659 (2020). https://doi.org/10.3390/s20092659

15. Walter, S., Schwanzer, P., Steiner, C., et al.: Mixing rules for an exact determination of the dielectric properties of engine soot using the microwave cavity perturbation method and its application in gasoline particulate filters. Sensors **22**, 3311 (2022). https://doi.org/10.3390/s22093311

16. Dietrich, M., Jahn, C., Lanzerath, P., et al.: Microwave-based oxidation state and soot loading determination on gasoline particulate filters with three-way catalyst coating for homogenously operated gasoline engines. Sensors **15**, 21971–21988 (2015). https://doi.org/10.3390/s150921971

17. Nicolin, P., Boger, T., Dietrich, M., et al.: Soot load monitoring in gasoline particulate filter applications with RF-sensors. SAE Tech. Pap. (2020). https://doi.org/10.4271/2020-01-2171

18. Sappok, A., Bromberg, L.: Radio frequency diesel particulate filter soot and ash level sensors: enabling adaptive controls for heavy-duty diesel applications. SAE Int. J. Commer. Veh. **7**, 468–477 (2014). https://doi.org/10.4271/2014-01-2349

19. Sappok A., Bromberg L., Parks J.E et al.: Loading and regeneration analysis of a diesel particulate filter with a radio frequency-based sensor. SAE Tech. Pap. (2010). https://doi.org/10.4271/2010-01-2126

20. Schwanzer P., Schillinger M., Mieslinger J. et al.: A synthetic ash-loading method for gasoline particulate filters with active oil injection. SAE Int. J. Engines **14** (2021). https://doi.org/10.4271/03-14-04-0029

21. Chen, P., Schönebaum, S., Simons, T., et al.: Correlating the integral sensing properties of zeolites with molecular processes

by combining broadband impedance and DRIFT spectroscopy-a new approach for bridging the scales. Sensors **15**, 28915–28941 (2015). https://doi.org/10.3390/s151128915

22. Chen, L.: Microwave electronics: measurement and materials characterization. Wiley, Chichester (2005)

23. Steiner, C., Walter, S., Malashchuk, V., et al.: Determination of the dielectric properties of storage materials for exhaust gas aftertreatment using the microwave cavity perturbation method. Sensors **20**, 6024 (2020). https://doi.org/10.3390/s20216024

24. Walter, S., Schwanzer, P., Hagen, G., et al.: Soot monitoring of gasoline particulate filters using a radio-frequency-based sensor. Sensors **23**, 7861 (2023). https://doi.org/10.3390/s23187861

25. Sethia, S., Kubinski, D., Nerlich, H., et al.: RF studies of soot and ammonia loadings on a combined particulate filter and SCR catalyst. J. Electrochem. Soc. **167**, 147516 (2020). https://doi.org/10.1149/1945-7111/abc83e

26. Feulner, M., Hagen, G., Hottner, K., et al.: Comparative study of different methods for soot sensing and filter monitoring in diesel exhausts. Sensors **17**, 400 (2017). https://doi.org/10.3390/s17020400

27. Sappok, A., Ragaller, P., Guarino, A., et al.: Direct measurement of aftertreatment system stored water levels for improved dew point management using radio frequency sensing. SAE Tech. Pap. (2019). https://doi.org/10.4271/2019-01-0739

28. Grünzweig, C., Mannes, D., Kaestner, A., et al.: Visualisierung der Russ- und Ascheverteilung in Dieselpartikelfiltern Mittels Neutronen-Imaging. Motortech. Z. **73**, 326–331 (2012). https://doi.org/10.1007/s35146-012-0440-0

29. Boger, T., Rose, D., Nicolin, P., et al.: Oxidation of soot (Printex® U) in particulate filters operated on gasoline engines. Emiss. Control Sci. Technol. **1**, 49–63 (2015). https://doi.org/10.1007/s40825-015-0011-1

30. Choi, S., Seong, H.: Oxidation characteristics of gasoline direct-injection (GDI) engine soot: catalytic effects of ash and modified kinetic correlation. Combust. Flame **162**, 2371–2389 (2015). https://doi.org/10.1016/j.combustflame.2015.02.004

31. Huynh C.T, Johnson J.H, Yang S.L et al.: A one-dimensional computational model for studying the filtration and regeneration characteristics of a catalyzed wall-flow diesel particulate filter. SAE Tech. Pap. (2003). https://doi.org/10.4271/2003-01-0841

32. Lupše, J., Campolo, M., Soldati, A.: Modelling soot deposition and monolith regeneration for optimal design of automotive DPFs. Chem. Eng. Sci. **151**, 36–50 (2016). https://doi.org/10.1016/j.ces.2016.05.008

33. Schwanzer P.: Experimentelle Untersuchungen zur On-Board Überwachung von Partikelfiltern für den Einsatz an direkteinspritzenden Benzinmotoren, pp. 117–131. Dr. Hut, München (2022)

34. Walter, S., Ruwisch, L., Göbel, U., et al.: Radio frequency-based determination of the oxygen and the NO_x storage level of NO_x storage catalysts. Top. Catal. **62**, 157–163 (2019). https://doi.org/10.1007/s11244-018-1079-y

35. Walter, S., Schwanzer, P., Hagen, G., et al.: Hochfrequenzsensorik zur direkten Beladungserkennung von Benzinpartikelfiltern. In: Tille, T. (ed.) Automobil-Sensorik 3, pp. 185–208. Springer Vieweg, Berlin (2020) https://doi.org/10.1007/978-3-662-61260-6_7